IEEE Access
Multidisciplinary ⋮ Rapid Review ⋮ Open Access Journal

Received 29 August 2023, accepted 14 September 2023, date of publication 18 September 2023,
date of current version 28 September 2023.

Digital Object Identifier 10.1109/ACCESS.2023.3316881

RESEARCH ARTICLE

A Study on the Fire Detection and Smoke Removal in Underground Utility Tunnel Using CFD

JEONG-HWA CHO[1], IN-BOK LEE[1,2,3], WOO-SUG JEONG[4], AND BYUNG-JIN LEE[4]

[1]College of Agriculture and Life Sciences, Research Institute for Agriculture and Life Sciences, Seoul National University, Seoul 08826, Republic of Korea
[2]Research Institute of Green Eco Engineering, Institute of Green Bio Science and Technology, Seoul National University, Pyeongchang, Gangwon-do 25354, Republic of Korea
[3]Department of Rural Systems Engineering, Global Smart Farm Convergence Major, College of Agriculture and Life Sciences, Research Institute of Agriculture and Life Sciences, Seoul National University, Seoul 08826, Republic of Korea
[4]Defense and Safety ICT Research Department, Disaster and Safety AI Convergence Center, Electronics and Telecommunications Research Institute, Daejeon 34129, Republic of Korea

Corresponding author: In-Bok Lee (iblee@snu.ac.kr)

This work was supported by the Electronics and Telecommunications Research Institute (ETRI) Grant by the Korean Government (Development of Integrated Platform Technology for Fire and Disaster Management in Underground Utility Tunnel Based on Digital Twin) under Grant 2020-0-00061.

ABSTRACT The underground utility tunnel is a facility for installing and managing public infrastructure such as electricity, water supply, and telecommunication, which are required for managing urban life. Due to the underground structure, airflow is different compared to general buildings, so heat and smoke are not smoothly removed in the event of a fire, making it difficult to evacuate safely of occupants and enter firefighters. Therefore, it is essential to accurately detect the fire location based on the current state of fire occurrence and to remove smoke efficiently. This study derived the optimum sensor location for detecting fire and exhaust fan operation for smoke removal by considering the ventilation system in the target underground utility tunnel. In the future, these results can be used as a response manual for underground facilities in case of fire. Analysis and understanding of how fire propagates inside critical infrastructures can prevent future accidents.

INDEX TERMS CFD, fire detection, fire safety, underground utility tunnel (UUT).

I. INTRODUCTION

An underground utility tunnel is an underground structure that jointly accommodates and supplies two or more facilities, such as electricity, gas, communication, and sewage. Since pipelines are buried in the ground to improve the aesthetics of the city and make the passage space more comfortable, the underground utility tunnel has been introduced mainly in new cities since the 2000s [1]. On the other hand, 12 out of 15 major underground utility tunnel disasters in Korea over the past 30 years are fire accidents [2]. Since the accident occurred in a space where social infrastructure facilities are built, a severe problem arises: the downtown area is paralyzed until the damage is restored. For example, in 2018, a fire broke out in the underground utility tunnel of the KT Ahyeon branch in Korea, and the internet and communication networks were cut off, so it was impossible to receive national guidance. There is also much damage worldwide due to the fire in the underground utility tunnel. For example, in 2012, 600 million people were blacked out by a transformer explosion in India. In 2017, the US airport in Georgia was suspended, and in 2022, three cities were blacked out in Hong Kong [3]. Accordingly, the Korea Fire Insurance Association established Fire Safety Standards for underground utility tunnels [2], a standard that provides the necessary safety standards to reduce the risk of fire that may occur in underground utility tunnels installed in buildings or sites. It is specified in the standard that at least one fire extinguisher should be installed for every 50 m of walking distance and 50 m^2 of floor area where electrical facilities are located. However,

The associate editor coordinating the review of this manuscript and approving it for publication was Agustin Leobardo Herrera-May.

it is difficult to respond to early fire extinguishing when a fire breaks out in the underground utility tunnel because of the long underground tunnel structure. Therefore, it is important to properly remove fire smoke to identify the exact fire location and to secure an evacuation route for occupants and an access route for firefighters for quick response.

Fire safety is a critical component of many installations because of the complexity involved in emergency evacuation and rescue operations. In addition, due to the long tunnel structure compared to existing buildings, underground utility tunnels cause more damage if proper fire prevention measures are not supported. Therefore, establishing systematic safety measures for underground utility tunnels, reviewing fire vulnerabilities, and preventing and suppressing fires have been mentioned in many studies [4], [5], [6], [7].

For fire prevention, measuring experimental data according to fire scenarios on a scale similar to the underground utility tunnel site is not easy. It requires a lot of human resources and manufacturing costs for experiments, and it is difficult to create uniform environmental conditions. However, numerical analysis methods such as Computational Fluid Dynamics (CFD) that analyze flow characteristics by simulating fires are being used. In addition, several studies have been analysed using the Fire Dynamics Simulator (FDS) to solve the Favre filter equation for mass, momentum, species mass fraction, and energy conservation in the CFD-based Large Eddy Simulation (LES) framework [8], [9], [10], [11], [12].

When a fire broke out in the underground utility tunnel, the structural design was changed to analyze the temperature distribution and flow velocity in various cross-sectional shapes or T- and L-shapes [13], [14], [15]. In addition, because hot air rises, the temperature and velocity of the fluid near the ceiling were analyzed by ventilation flow rate and mode conditions [16], [17]. The results of the studies indicated that proper mechanical ventilation was adequate compared to typical road fires. In addition, a study on the heat distribution characteristics related to fire in an underground facility, which is an environment similar to an underground utility tunnel, was conducted. Several underground facilities were targeted as follows: cabin [18], subway [19], tunnel [20], [21], [22], [23], [24], platforms [25], mines [26], railways [27], parking lots [28]. These studies aimed to analyze fire risk and design response scenarios by predicting heat flow, temperature distribution, and gas diffusion when a fire breaks out. Methodologies proposed to prepare countermeasures against fire include optimized heat and smoke detectors, automatic fire suppression, and smoke exhaust systems. If the fire occurrence and the location of the fire source are quickly detected, evacuation can be made safely, and the time required for the combustion process can be shortened. So, typical buildings are equipped with automatic detectors and fire suppression systems [29]. In other words, effective smoke exhaustion is essential to fire safety performance. Due to the smoke generated by the fire, visibility affects evacuation movements, and it is the indirect but fatal cause of death for evacuees to be trapped in the early stages of the fire [30]. Since it is difficult to build an automatic fire suppression system in underground utility tunnels due to its structure, studies focusing on fire detection and smoke removal have been conducted.

For fire detection in underground utility tunnels, Jeongsoo et al. [31] proposed a deep learning-based fire detection model by comparing and analyzing fire data of the general sites and an environment similar to underground utility tunnels. Baalisampang et al. [32] analyzed the fire detector activation time by analyzing the smoke movement speed according to the distance from the fire boundary. Byung-Jin et al. [33] developed a sound-based deep learning model by detecting the sparking sound in advance because there is a blind spot of monitoring Closed-circuit Television (CCTV) and difficulties in processing many image data. In addition, several smoke removal studies have been conducted in the event of a fire in an underground utility tunnel based on CFD simulation. Willemann and Sanchez [34] have derived simulation results for various ventilation methods in case of an actual fire to determine the optimal ventilation design to control the smoke spread and prevent back layering. Yoo [22] calculated the temperature at the center in the width direction according to the damper's opening in the event of a tunnel fire. They designed a fire response scenario for a partial smoke exhaust system that increases smoke efficiency. kyu [35] and Dongkyu et al. [6] reviewed the domestic, Japanese, and US design standards for underground utility tunnels to derive the appropriate airflow velocity to secure smoke removal performance, compared them with actual measurements, and derived the optimal airflow velocity. Wang et al. [36] studied the effects of various ventilation methods and fire locations on the smoke diffusion characteristics of gas cabins in underground utility tunnels. They provided guidelines for the design, operation, and maintenance of ventilation in underground utility tunnels. Baalisampang et al. [37] optimized the smoke exhaust system by evaluating the difficulty of emergency evacuation through the corridor and confirming the importance of securing visibility.

However, as the studies were conducted only for a short section of about 100 to 200m [36], [38], [39], existing research methods for controlling fire detection or smoke spread have limitations. It is difficult to understand the characteristics of high-temperature heat flow distribution over the entire area of a long underground utility tunnel. In addition, when the forced ventilation fan is operated to remove smoke, the ventilation characteristics against the natural force caused by buoyancy due to the various inclined structures of the underground utility tunnel were not considered. Therefore, it is necessary to analyze the airflow during a fire for the entire section of the long utility tunnel with the exhaust fan operating according to the conditions.

In this study, airflow was analyzed considering the ventilation system of the target utility tunnel to detect fire

location and efficiently remove smoke. A 3-dimensional CFD model was designed and validated for fire simulation analysis considering the air conditioning system of the target underground utility tunnel [40]. The model evaluated the minimum sensor installation distance spacing for fire detection. Finally, a proper ventilation operation for smoke removal was proposed. The target section of this study was selected for the section of the electricity compartment that is relatively vulnerable to fire due to the arrangement of power lines and the section with complex structures, including stairs in the target underground utility tunnel. The fire was limited to a 1MW scale [41], which is the standard for fire growth, and a steady-state in which the fire was sufficiently spread was assumed. That is, the spread of the fire was not considered, and the study was conducted on the role of the ventilation system in fire detection and smoke removal. Accordingly, it will be possible to establish a ventilation system operation plan for efficient smoke control in the event of a fire in a long section, such as an underground utility tunnel. It can be used as a resource to help evacuate occupants or secure an access road for firefighters.

II. MATERIALS AND METHODS

Figure 1 shows the flow chart of this research process. The optimal number of sensors for detecting the location of fire sources in a target underground utility tunnel was analyzed. And an operation plan for operating an exhaust fan to diffuse and remove generated smoke only in the minimum section was to be derived. If the smoke-spreading section is long, it is difficult for residents to evacuate safely and for firefighters to enter, so only the minimum section was spread. Furthermore, unlike general buildings on the ground, the underground utility tunnel does not have solar radiation, and airflow is not smooth. So, smoke was removed by forced ventilation according to the operation of the ventilation system installed inside and the buoyancy of the high-temperature smoke caused by the fire. So, ventilation is achieved by buoyancy due to high-temperature smoke and by forced ventilation according to the operation of the ventilation system installed inside.

A field experiment was conducted to simulate the primary air flow according to the gradient structure and the internal and external temperature difference before a fire broke out in the underground utility tunnel. Ventilation amount and wall surface temperature were measured according to exhaust fan operating conditions. Fan operating conditions were different for each season in the underground utility tunnel on site. During the summer, all fans are turned on when the fan is running.

In winter, the fan is not always operated. When the exhaust fan is operated, the fire model was simulated by inputting the fan flow rate measured at the site. When the exhaust fan is not operated, the buoyancy effect is generated by natural convection. Prior to simulating the fire, the tendency of smoke diffusion inside the utility tunnel was calculated at regular times when there were no fires. When a fire was simulated, the location of the fire source was assumed in detail in the section with a complicated structure. Basically, the fire sources located at three intervals between the inlet and outlet vents were compared for each season and for each exhaust fan operating condition. According to these conditions, the temperature difference was estimated to properly detect the fire location by season.

The sensor detection distance for each section was calculated based on the temperature difference. As a result, the number of sensors was derived through the minimum detection distance for each section. Using the derived number of sensors, sensor detection results were derived for each season and fan operation. The operating condition of the exhaust fan that diffuses and removes the smoke only in a short section was derived.

A. TARGET UNDERGROUND UTILITY TUNNEL

The target utility tunnel is located in Korea and the total length of the facility is about 2,400m, and is divided into a water pipeline, a telecom, and an electricity compartment. (Figure 2 (a)) The gradient of the target section is shown in Figure 2 (b). The depth was indicated by the location between the deepest vents 6 and 7. The experimental site of this study has a depth difference of more than 30 m from the deepest bottom. In the study area, including vents 6 to 10, the section after vent 7 has a single upper gradient considering drainage and the same depth shape as the site was modeled to examine heat flow by natural convection in case of fire. In addition, the same shape was implemented for the perforation of the bulkhead installed for ventilation in the section divided into three compartments. The stairway between ventilators 6 and 7 was also implemented in the same shape as the real one.

Most fire accidents in underground utility tunnels in Korea were caused by electrical short circuits and negligence in welding, which caused fires in the section at telecom and electricity compartments. As shown in Figure 2 (c), of the total 15 vents, the ventilation system of the vents 6 to 10, which are the target section, have a total of 3 outlet and 2 inlet vents installed alternately. It is a negative pressure ventilation structure in which air is supplied by a natural air supply and exhausted by mechanical ventilation. Based on the temperature value measured by the Resistance Temperature Detectors (RTD) sensor installed near the exhaust fan, the exhaust fans are automatically operated when the internal temperature is 25°C or higher or 80% relative humidity, and manually.

B. FIELD EXPERIMENT

Since the amount of ventilation significantly affects the control of the internal air environment, the capacity of the exhaust fan installed in vents 6 to 12 was measured. To measure the ventilation flow rate of the exhaust fan, it was difficult to use an air flow meter, so a hot wire anemometer was used. Because the exhaust fan has a mesh net installed on the cross-section of the exhaust side, and thus the pipe flow is broken. Furthermore, when the flow volume hood is installed

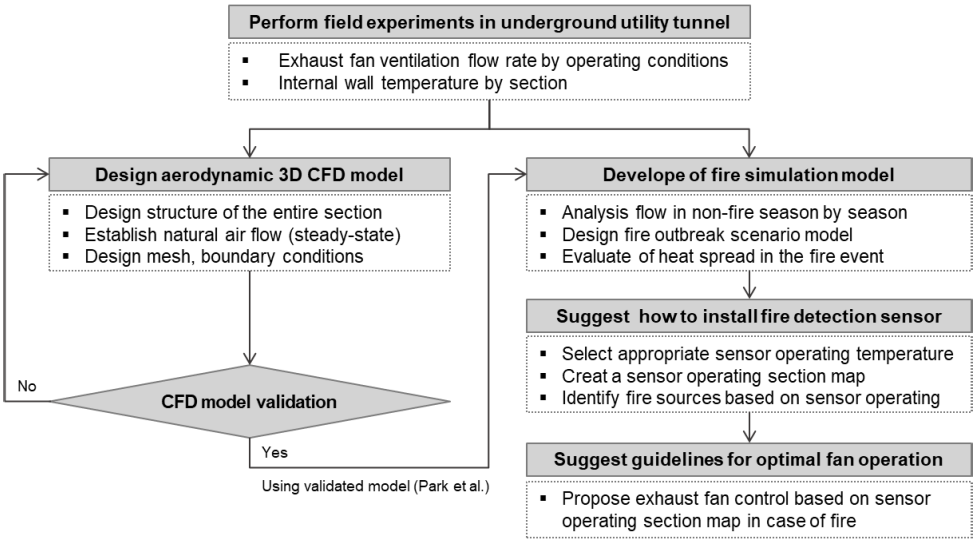

FIGURE 1. Flowchart of the research procedure.

for air flow meter, a distance of less than 50 cm from the side wall of the external structure is insufficient. Therefore, considering the field conditions, the 1-minute average flow velocity was measured for the inlet section of the exhaust fan using a hot-wire anemometer (TESTO 480, Testo, Germany), and multi-point was measured.

On the other hand, in the target utility tunnel, inlets and outlets are installed alternately, so the air introduced from the adjacent inlet is discharged through the exhaust fan. Since the amount of air flowing in from the adjacent inlets may vary between the condition in which the exhaust fan was operated alone and the condition in which the surrounding fan was simultaneously operated, the exhaust fan flow rate was measured for both conditions. In addition, the surface temperature of the inner wall of the utility tunnel, which affects the air environment of each section of the target underground utility tunnel, was measured with a thermal imaging camera (FLIR E5, Flir, USA). (Figure 3).

C. COMPUTATIONAL FLUID DYNAMICS

Computational Fluid Dynamics (CFD) is a tool that can analyze fluid flow, heat transfer, and chemical reactions in physical systems containing fluids. CFD simulates numerical analysis using the nonlinear differential equation, the Navier-stoke equation, as the governing equation and using the finite difference method. It is actively used in various fields, including mechanical, aerospace, chemical engineering, manufacturing, civil and architectural, and environmental fields [42], [43], [44], [45], [46]. In this study, a 3D grid was designed using a CFD commercial program (Fluent, Ver. 19.2 ANSYS Inc.) to propose an appropriate fan operation plan for position detection and smoke removal in case of fire in the utility tunnel. Boundary conditions were set, and calculations were performed for the designed target space. The mass, momentum, and energy conservation equations used in the calculations are as follows: equation (1 - 3).

$$\frac{\partial \rho}{\partial t} + \nabla \cdot (\rho \vec{v}) = S_m \tag{1}$$

$$\frac{\partial}{\partial t}(\rho \vec{v}) + \nabla \cdot (\rho \vec{v}\vec{v}) = -\nabla P + \nabla \tau + \rho \vec{g} + \vec{F} \tag{2}$$

$$\frac{\partial}{\partial t}(\rho h) + \nabla \cdot (\vec{v}(\rho h + P)) = \nabla \left(k_{eff} \nabla T - \sum_j h_j \vec{J}_j + (\vec{\tau}\vec{v}) \right) + S_h \tag{3}$$

where, ρ is the density of the fluid (kg/m^3), $\vec{v}$ is the flow velocity of the fluid (m/s), P is the static pressure (Pa), $\vec{\tau}$ is the stress tensor (Pa), and $\vec{g}$ is the acceleration due to gravity. (m/s^2), $\vec{F}$ is the external force (N/m^3), S_m is the mass source generated by a chemical reaction (kg/m^3), k_{eff} is the effective conductivity (kg/m^2·s), T is the temperature (K), E is the specific enthalpy indicating the enthalpy per unit mass (J/kg), t is the time (s), $\vec{J}_i$ is the diffusion flux of i type (kg/m·s), S_h is the enthalpy rise based on the chemical reaction or radiation (kg/m·s^3).

D. DESIGN OF THE CFD MODEL FOR THE FIRE SPREAD

1) MODEL VALIDATION

In this study, the validation model built in the study of Park et al. [40] was used to secure the reliability of the fire analysis CFD model. The structural information of the CFD model was designed using the LiDAR model, and the entire section was implemented to simulate the airflow through each inlet and outlet. The mesh was composed of about 800,000 cells using a hexahedral mesh, and the volumes of the minimum and maximum mesh were 7.05E-06 and 1.15E-01 m^3, respectively, and the minimum skewness was 0.72. The internal ventilation system was

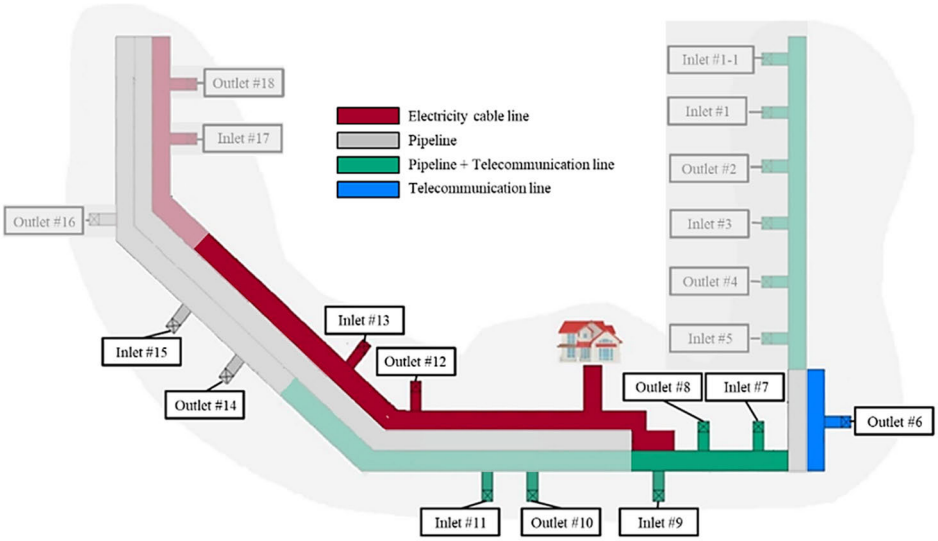

(a)

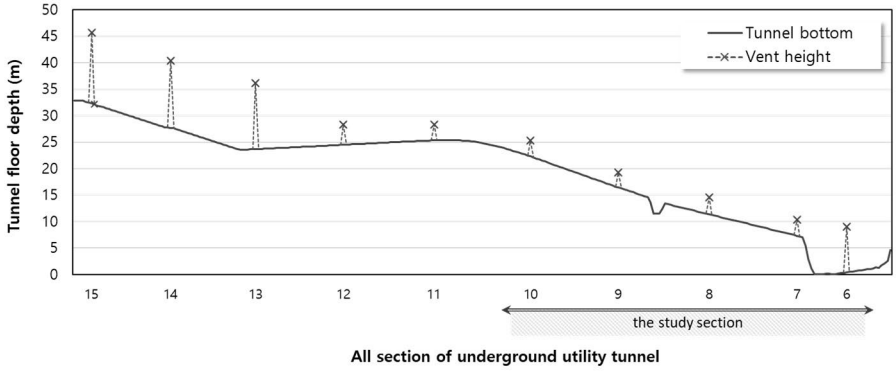

(b)

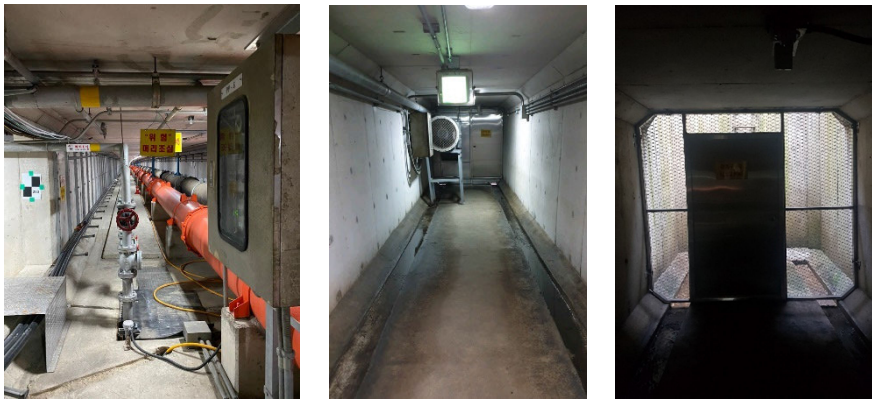

inside the tunnel outlet vent inlet vent

(c)

FIGURE 2. Schematic diagram and drawing cross section of underground utility tunnel: (a) Schematic diagram (b) Drawing of cross section (c) Internal tunnel and vents view.

identically implemented, and when the ventilation fan was operated, the model was validated using experimental field values.

First, when the exhaust fan at vent six was operated, the air velocity simulated value was compared with the experimentally measured value. As a result of validation, the standard k-ε model showed high accuracy of $R^2 = 0.96$ and Root Mean Square Error (RMSE) = 0.13, so the corresponding turbulence model was used. (Figure 4) The accuracy of this model is highly recognized, and the literature is the most abundant [47], [48], [49], [50], [51]. Next, the air temperature at each outlet was validated by considering the seasonal ventilation fan operation of the utility tunnel. In the case of exhaust fan operating conditions in summer, the simulated

FIGURE 3. Flow velocity and wall surface temperature measurement experiment: (a) Ventilation flow rate measurement at the inlet of exhaust fan (b) Wall surface temperature measurement for each tunnel section.

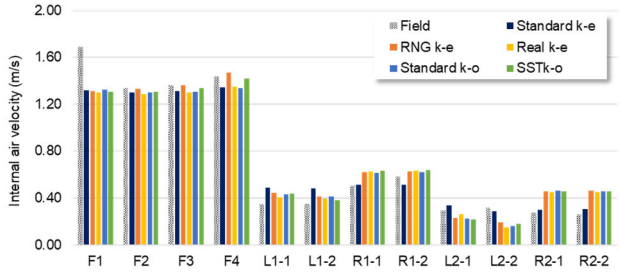

FIGURE 4. Comparative analysis of the internal flow velocity according to the application of turbulence models (Park et al. 2022).

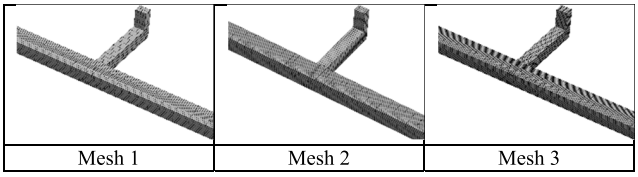

FIGURE 5. Typical mesh structure used for CFD simulations.

and measured values for each outlet showed a difference of 0.47 ∼ 4.06 °C.

However, the tendency to discharge the accumulated heat from the nearby electricity compartment was the same. In the case of the exhaust fan not operating in winter, the simulated and measured values showed a slight difference of 0.0 ∼ 1.7 °C depending on the tunnel section. Seasonal simulated results showed the same tendency for temperature distribution compared to field experiment value, representing that the air inflow and outflow through the vent of the utility tunnel is calculated the same as that of the field. The model was validated using the field measurement results, and the fire outbreak in the underground utility tunnel was simulated using a reliable model.

2) MESH INDEPENDENCE TEST

The accuracy of the approximation calculation result varies depending on the degree of lattice division of the model. The number or size of grids for optimal grid design is analyzed through a grid independence test. For the test, the analysis space was selected around the space where the fire occurred in the underground utility tunnel. In the case of fire, heat was applied to extract values in the longitudinal direction, and pressure, speed, and temperature results were compared. It was calculated for each condition from the coarsest mesh to determine the optimal mesh density. It was divided into mesh 1 (15,000 cells), mesh 2 (54,500 cells), and mesh 3 (163,000 cells) conditions between vents 7 and 8 (Figure 5). If the mesh is configured more densely, the computation time increases rapidly, making the computation time less economical. The error percentage between mesh 2 and mesh 3 was analyzed as 2.77%, 2.75, and 2.11% in the order of pressure, velocity, and temperature. The mesh condition that secured independence by comparing the calculation results was determined as mesh 2 and defined as the optimal grid condition.

3) BOUNDARY CONDITIONS DESIGN

The density gradient occurs, resulting in a buoyancy effect in which the hot air moves upward due to the air temperature inside and outside the underground utility tunnel and the inclined structure. So natural convection flows even when the exhaust fan is not operated. In summer, the high temperature outside air enters the inlet, some of which are stored underground wall, so some heat is removed from the inside of the underground utility tunnel. During winter, low-temperature outside air is introduced, releasing heat from the wall. The average value of surface temperature measurements of the side walls, ceiling, and floor for each distance from the inlet using a thermal imaging camera was input as a boundary condition. Table 1 shows the final design specifications and boundary conditions of the CFD simulation model used in this study. In order to analyze the overall trend of the smoke spread after a fire has sufficiently occurred, it was calculated as a steady state. The SIMPLE (Semi-Implicit Method for Pressure Linked Equations) algorithm was used, which provides flexibility in the analysis procedure and has good convergence. In addition, pressure conditions were entered into each vent, as shown in Table 2, to create conditions corresponding to the temperature measured in the field experiment. It was assumed that the exhaust fan of vents 6, 8, 10, and 12 operated in the summer as in the field, and all vents were naturally ventilated in the winter.

4) CASE ANALYSIS

First, input values were selected to reflect the common flow conditions according to seasonal compared to the field measurement results for regular times. Based on the results for regular times, it was possible to secure the reliability of the simulated results interpreted for virtual fires. And then, the effect of the ventilation system was evaluated seasonally to analyze the flow of high-temperature air formed when a fire broke out in the underground utility tunnel. Assuming that the intensity of the fire was 1MW, the temperature characteristics of each section were evaluated.

TABLE 1. Design conditions of simulation models.

Conditions	Value
Time step	Steady state
Solver	Pressure based
Spatial discretization of momentum, volume fraction, turbulent kinetic energy, and turbulence dissipation rate	Second-order upwind
Spatial discretization of gradient	Least squares cell-based
Inlet temperature	32℃ (Summer), 0℃ (Winter)
Convergence criteria	1×10^{-6} (energy), 1×10^{-3} (other)
Air density	Incompressible-Ideal gas
Gravitational acceleration	9.81 m/s^2

TABLE 2. Pressure per vent when exhaust fan is not operating.

Vent	6	7	8	9	10	11	12	13	14	15
Pressure (Pa)	3.00	4.00	1.00	3.87	-2.00	-1.80	-2.13	-2.43	-1.49	0.00

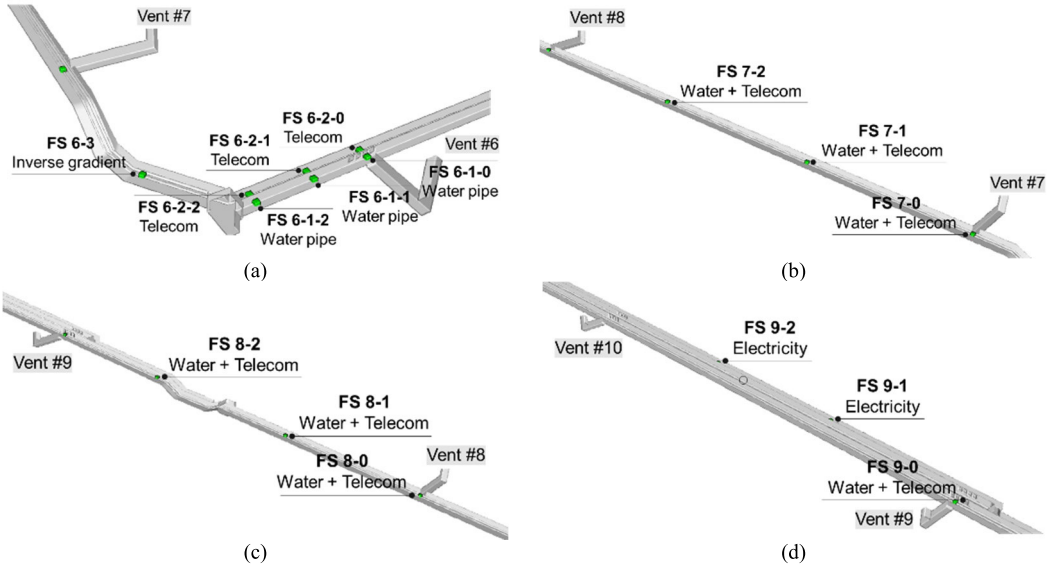

FIGURE 6. Location of fire sources by vent section: (a) Vent 6 ∼ 7 (b) Vent 7 ∼ 8 (c) Vent 8 ∼ 9 (d) Vent 9 ∼ 10.

TABLE 3. Number of cases analyzed in this study.

Classification	Conditions	Number of cases
state	fire/ not fire	2
fire source location when simulated fire	from 6-1-0 to 9-3	16
season	Winter / Summer	2
fan operation	working / not working	2

1MW is a level of the fire growth rate as a standard for determining flashover, a phenomenon that rapidly and instantaneously burns combustibles indoors after the fire growth stage. According to the standards specified by the National Fire Protection Association (NFPA) of the United States, fire stages are classified according to the time for the Heat Release Rate (HRR) to reach 1 MW in calorific value when a fire occurs [41]. This was selected only for the scale and cases that could occur in the underground utility tunnel. It was also assumed that the smoke spread of a fire is similar to the high-temperature spread trend [15], [25], [52]. The location of the fire source was analyzed, as shown in Figure 6. Vent 6∼7 section has a gradient change. A total of 7 locations were analyzed, 2 locations each (6-1-0 ∼ 6-2-2) since the telecom and water pipelines compartments are partly double-tracked, and 1 location (6-(3) at the upper gradient location where the two utility tunnels were combined. In the vent 7 to 10 section, the third division between each vent was

TABLE 4. The measured ventilation flow rate of the exhaust fan.

Fan	Operating condition	Inlet air velocity (m/s)	Measured ventilation flow rate (CMM)	Specification (CMM)
6	single (6)	7.01	255.8	27
	all nearby (4, 6, 8)	7.16	261.1	
8	single	6.28	96.1	72
	all nearby	5.78	88.5	
10	single	14.53	307.3	340
	all nearby	15.14	320.3	
12	single	13.92	294.5	340
	all nearby	13.36	282.71	

TABLE 5. Wall temperature distribution when winter fan is not operating.

Vent	Location	Floor	Side	Ceiling	Floor	Side	Ceiling	Floor	Side	Ceiling
6	length		0m			25m			50m	
	left	4.5	6.7	7.4	7.3	8.6	9.7	7.5	8.0	8.2
	right	5.9	8.0	8.5	7.5	9.0	9.0	7.7	8.8	8.3
7	length		0m			45m			105m	
	left	2.3	3.5	4.1	5.2	4.0	5.0	6.1	5.2	5.8
	right	2.5	3.8	4.7						
8	length		0m			55m			100m	
	left	6.4	6.4	6.0	7.5	7.3	6.8	7.5	8.0	8.0
9	length		0m			50m			100m	
	left	3.8	5.5	5.0	6.0	6.1	5.8	7.2	6.8	6.2
	middle	4.4	5.0	4.2	6.2	5.8	5.5	7.2	6.8	6.2
	right	3.3	4.0	5.2	6.0	7.5	6.0	8.0	9.4	7.7
10	length		0m			50m			100m	
	left	7.5	6.6	6.2	7.5	6.6	6.1	7.9	7.0	6.9
	middle	7.1	7.0	6.3	7.6	6.8	6.2	6.2	8.0	7.0
	right	8.2	9.6	8.0	8.8	11.0	9.0	10.2	11.0	8.0
11	length		0m			50m			100m	
	left	8.0	6.5	6.8	8.0	7.2	7.0	8.1	7.7	6.9
	middle	8.0	7.6	7.0	8.3	8.0	7.5	8.6	8.4	7.5
	right	10.0	11.0	9.7	10.0	12.4	9.8	11.7	12.5	10.2
12	length		0m			50m			100m	
	left	8.5	8.0	7.2	8.2	7.9	7.3	8.3	7.8	0.5
	middle	8.1	8.3	7.1	8.6	8.4	7.6	8.7	8.2	7.6
	right	9.0	13.0	9.9	10.8	12.0	9.8	11.0	12.0	9.8
13	length		0m			45m			85m	
	left	7.8	7.4	9.0	8.4	8.0	9.2	8.5	8.0	5.2
	middle	8.3	8.0	7.2	9.3	9.8	8.7	10.4	11.0	9.6
	right	9.7	12.7	9.0	11.7	13.8	11.8	15.0	19.0	15.1
14	length		0m			45m			85m	
	left	5.2	7.6	7.5	9.2	8.1	8.0	9.0	8.2	7.7
	middle	8.7	10.8	9.7	10.0	11.5	10.0	10.3	11.4	9.3
	right	10.5	16.6	13.6	14.2	18.8	15.8	11.0	19.5	16.0

TABLE 6. Comparison of measured and calculated air temperature values according to seasonal fan operation (°C).

(a) Summer, fans working

Fan	Measured	Calculated
6	19.70	19.23
8	-	20.22
10	22.45	20.98
12	26.68	24.75
14	23.67	19.61

(b) Winter, fans not working

Fan	Measured	Calculated
6	7.5	7.5
8	6.3	5.1
10	6.8	5.1
12	7.9	8.9
14	6.8	7.8

selected as the location of the fire source. Due to the nature of the underground space, airflow is not smooth compared to general ground buildings, so heat, and smoke cannot be removed smoothly in the event of a fire, making it difficult to evacuate safely of occupants and to enter firefighters. So, to accurately detect the fire location, the operating range of the detection according to the rapid temperature difference compared to regular times was studied. The fire location was

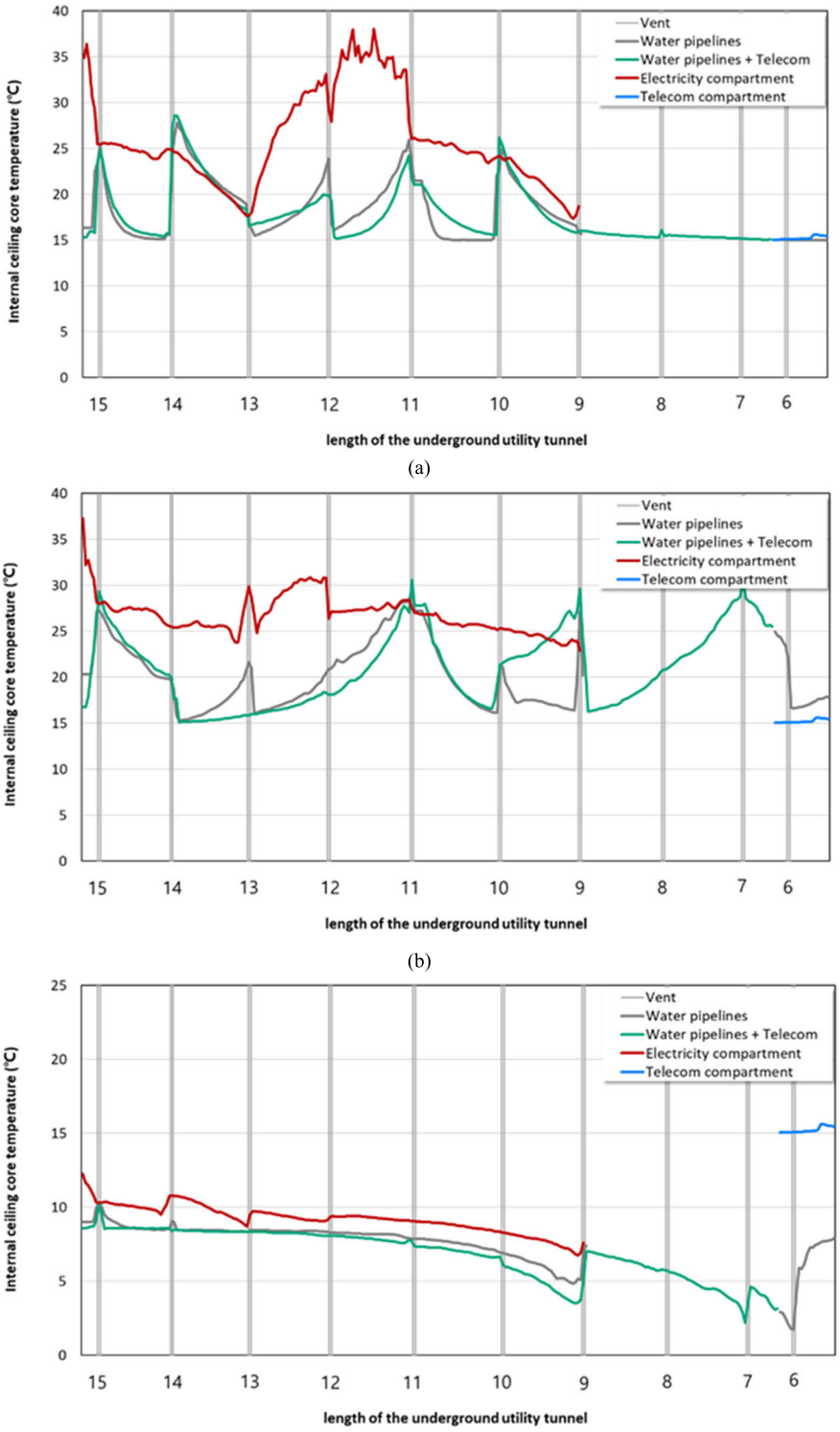

FIGURE 7. Air temperature distribution inside the underground utility tunnel according to seasonal fan operation in normal times: (a) Summer, fans working (b) Summer, fans not working (c) Winter, fans working (d) Winter, fans not working.

detected by analyzing the high-temperature smoke spread based on the temperature of the central part of the ceiling of the utility tunnel. According to KFS-1252 [2], it is specified that an automatic fire detection sensor must install a detector that can identify the ignition location within a 5 m margin of error. However, since the length of utility tunnels in Korea

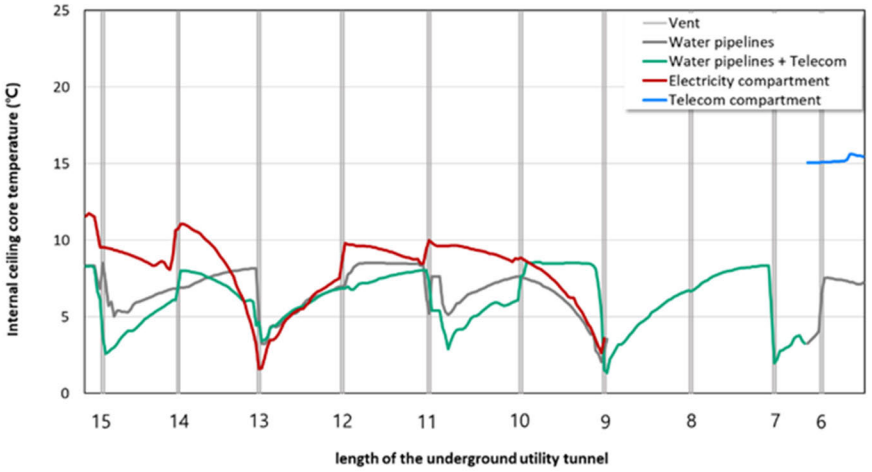

(d)

FIGURE 7. *(Continued.)* **Air temperature distribution inside the underground utility tunnel according to seasonal fan operation in normal times: (a) Summer, fans working (b) Summer, fans not working (c) Winter, fans working (d) Winter, fans not working.**

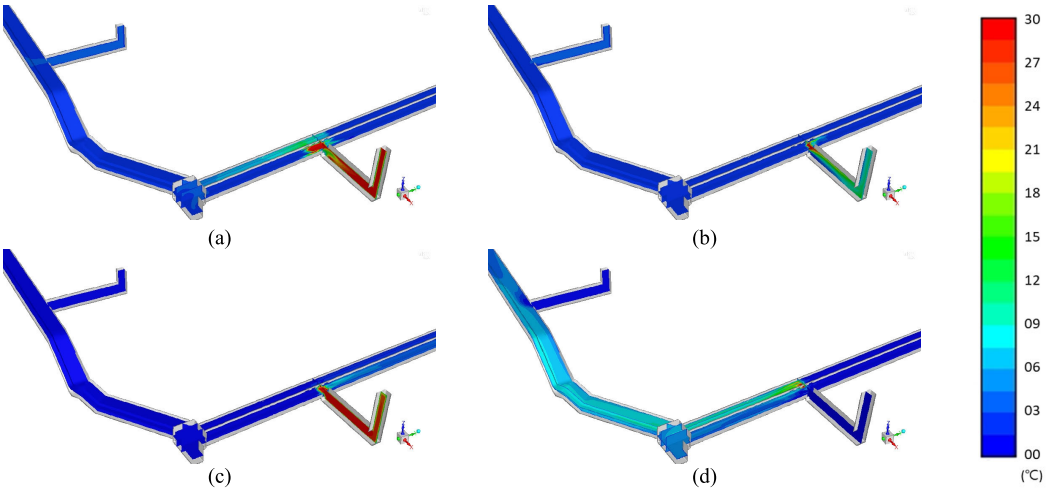

FIGURE 8. **Air temperature distribution inside underground utility tunnel in case of fire source at 6-1-0: (a) Summer, fans working (b) Summer, fans not working (c) Winter, fans working (d) Winter, fans not working.**

TABLE 7. **Assessment of the number of sensors for each section.**

Section between vents	6 ~ 7	7 ~ 8	8 ~ 9	9 ~ 10
Minimum sensor working distance (m)	15	150	75	270
Suggested sensor spacing (m)	7.5	75	37	135
Distance between vent (m)	60	150	153	150
Number of sensors	8	2	5	2

is several kilometers, such as 131 km for the electricity compartment and 281 km for the telecom compartment, problems in terms of malfunction and cost management may occur due to excessive installation of sensors when the standard is applied. The fire simulation calculated the air temperature at 5 m intervals along the central part of the ceiling to analyze the thermal behavior of high-temperature air.

The fire simulation, simulated the air temperature at 5m intervals along the central part of the ceiling to analyze the thermal behavior of high-temperature air.

Meanwhile, according to the fire safety standard for automated fire detection announced by the National Emergency Management Agency [53], it is stated that it would be appropriate to install a sensor with high adaptability among sensors

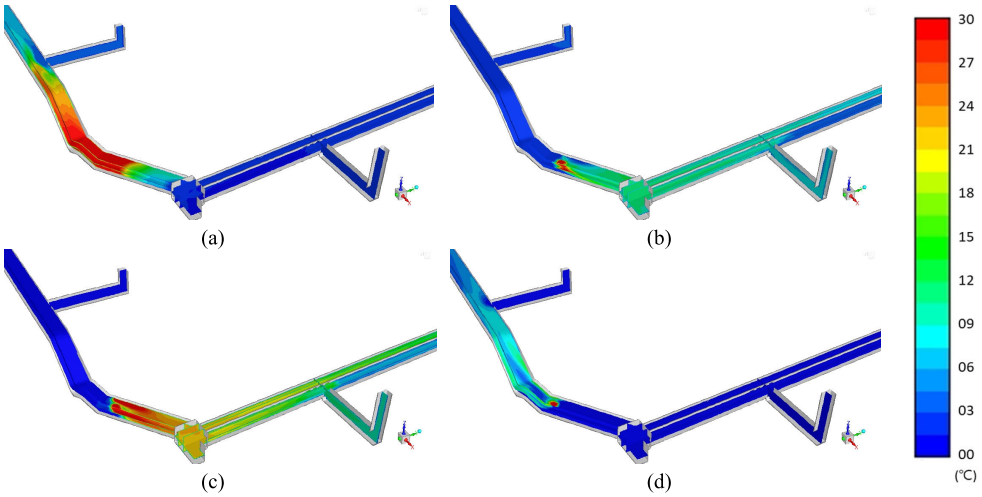

FIGURE 9. Air temperature distribution inside underground utility tunnel in case of fire source at 6-3: (a) Summer, fans working (b) Summer, fans not working (c) Winter, fans working (d) Winter, fans not working.

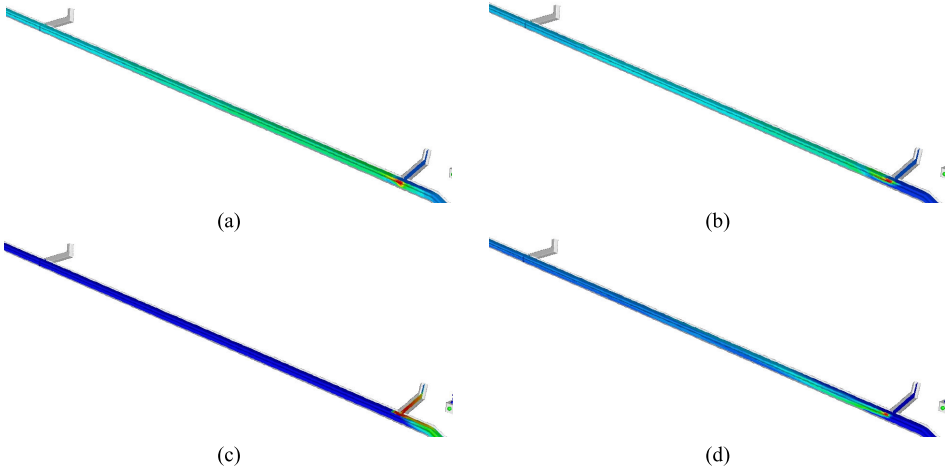

FIGURE 10. Air temperature distribution inside underground utility tunnel in case of fire source at 7-0: (a) Summer, fans working (b) Summer, fans not working (c) Winter, fans working (d) Winter, fans not working.

in places where ventilation is poor or where the distance between the sensor attachment surface and the indoor floor is less than 2.3m in the basement. Since the air temperature varies according to the season for each section regular times, a sensor that detects when the temperature exceeds a specific temperature was selected. Also, it is specified that the nominal operating temperature at which the detection sensor operates is 20 °C higher than the maximum ambient temperature. Therefore, it was assumed that a fire was detected when the temperature rose by 20, 40, and 60 °C, respectively, by comparing the air temperature difference between non-fire and fire. In order to accurately determine the location of the fire source, the appropriate fire detection temperature and spacing were calculated by analyzing each condition.

Ventilation methods for smoke removal in case of fire were simulated under the condition of simultaneously operating all exhaust fans or stopping in the event of a fire being detected. This presents the most uncomplicated operating conditions to reduce human error since operating the exhaust fan individually has a risk of causing an operator's mistake in an emergency. In addition, exhaust fan operating conditions in which high-temperature smoke is exhausted to the nearest vent and prevented from spreading to adjacent sections were evaluated. Finally, an effective method of spreading and distributing smoke only in a short section was determined and presented.

The number of simulation analysis cases was designed, as shown in Table 3, for fire detection and efficient smoke removal in case of fire in the underground utility tunnel. It was analyzed according to the operation of the fan by season by dividing the regular time and the time of the fire, and in the case of a fire, there are a total of 16 fire source locations targeting the vent 6-10 sections. The seasons were typically considered for summer and winter. In addition, whether to

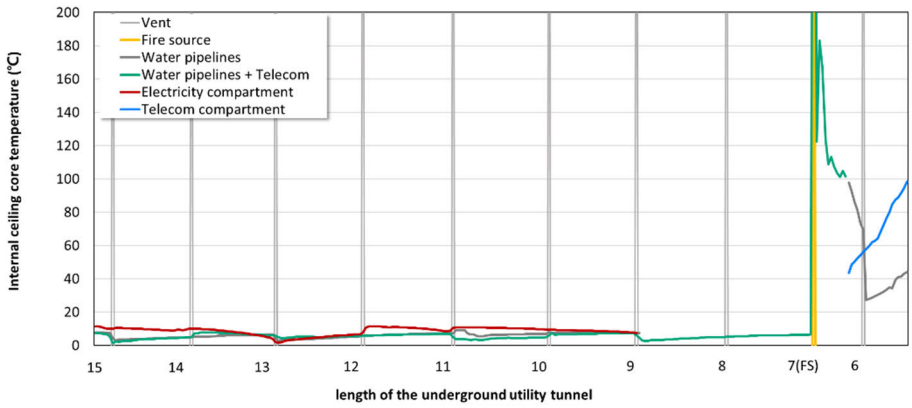

Vent	15	14	13	12	11	10	9	8	7	6
VFR (CMS)	6.87	-5.04	6.13	-4.71	4.89	-5.34	4.89	-1.47	-1.46	-4.35
Temp (℃)	0.00	4.97	0.00	6.03	0.00	4.95	0.00	5.51	36.15	43.43

(a)

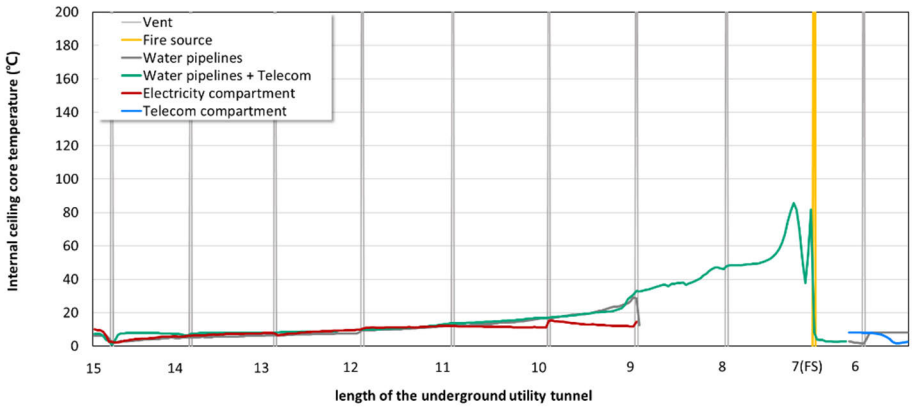

Vent	15	14	13	12	11	10	9	8	7	6
VFR (CMS)	5.87	-1.34	-3.66	-4.54	-5.00	-4.70	3.13	-2.36	6.74	4.96
Temp (℃)	0.00	6.61	7.30	9.15	13.13	16.53	0.00	17.35	0.00	0.00

(b)

FIGURE 11. Internal ceiling core temperature in case of fire source at 7-0: (a) Winter, fans working (b) Winter, fans not working.

operate exhaust fans was considered for the conditions under which all exhaust fans were operated or turned off. It was simulated for a total of 68 cases.

The simulations were run on a high-performance computer (HPC), each with two six-core Intel Xeon CPUs and 16 GB of memory. For simulations, eight processors of the HPC were used. The approximate run time to reach a steady state was 1∼2 days.

III. RESULTS AND DISCUSSIONS

A. FIELD EXPERIMENT RESULTS

Table 4 shows the experimental results of measuring the flow rate of each exhaust fan installed in the underground utility tunnel. The exhaust fan flow rate was measured for the summer when the exhaust fan was operating. For most exhaust fans, the ventilation flow rate was lower than the specification, and a value greater than the specified flow rate was measured only for exhaust fan 8. When the fan near the exhaust fan was operated, the measured flow rate was less than the design flow rate in general. This is because the air flow in duct is broken because the exhaust fan is connected to the outside by a duct, and the mesh net is installed at the end. In addition, it is analyzed that the exhaust outlet is blocked by the vertical tunnel structure of the vent, and the reason is due to the aging of the fan. This is the result of measuring the surface temperature of the inner wall of the target underground utility tunnel with a thermal imaging camera. (Table 5) The temperature difference between the floor, side walls, and ceiling was similar, within 0.7 °C on average, but the average temperature of the wall between the vents showed a significant difference with a maximum

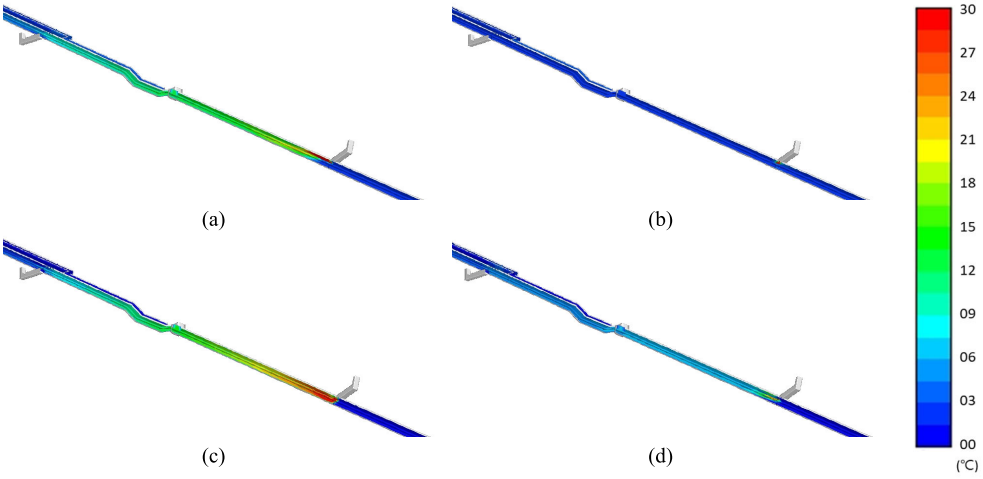

FIGURE 12. Air temperature distribution inside underground utility tunnel in case of fire source at 8-0: (a) Summer, fans working (b) Summer, fans not working (c) Winter, fans working (d) Winter, fans not working.

of 6.4 °C. This is judged to be the difference according to the internal heating value of the power conduit and the water conduit, and this can affect the air heat environment of each section of the underground utility conduit, so it was set as an input value as a boundary condition in the model.

B. THERMAL ANALYSIS IN NON-FIRE AND FIRE CONDITIONS

In order to reflect the flow conditions that occur, the measured values under operating conditions at regular times and calculated values were compared. As for normal operating conditions, it was assumed that the exhaust fan was operated for each season in the same way as the field. As shown in Table 6, the average value was measured for one year, from November 2019 to October 2020. The simulated value showed a difference of 0.47 ∼4.06 °C for each section when the fan was operating in summer. From vent 10, there is an internal heat gain of the wire to the electricity compartment section, so the temperature at the inlet is lowered. In addition, when the ventilation fan is not operating, it can be seen that the outside air has a higher temperature than the inside is introduced, and the internal temperature rises. (Figure 7) In winter, the average temperature difference between the measured value and the simulated value was 0.98 °C under the condition of ventilation by natural convection at regular times. In addition, it can be seen that the temperature of the vent through which the outside air flows is shallow because the inside temperature is higher than the outside air temperature.

Next, the heat diffusion flow was analyzed in the event of a fire in the underground utility tunnel. To this end, the air temperature contour was shown for each section, and, if necessary, the air temperature at the top of the ceiling was shown. The volume flow rate of each vent was presented by indicating the positive value as the supply through the vent and the negative value as the exhaust through the vent. If the fan is operated in a fire source 6-1-0, high-temperature smoke from the fire is discharged to vent 6, and in the summer, even if the fan is not operated, there will be no spread of smoke to sufficient exhaust. However, in the winter, low-temperature outside air comes in through vent 6, and the maximum temperature is relatively low. If the ventilation fan is not operated, all vents 10 to 13 act as outlets, flowing in the direction of vent 7, which is a low gradient, and there is a risk that fire smoke will spread to vent 7. (Figure 8) In the event of a fire at the location, it is analyzed that the operation of the ventilation fan is necessary regardless of the season to prevent smoke from spreading.

The thermal behavior in the 6-1-1 fire source is similar to that of the previous 6-1-0. However, the capacity of exhaust fan 6 is insufficient, so the high-temperature smoke spreads in the direction of vent 5 through vent 6. Most of the 6-1-0 fire sources are naturally exhausted to the vent before the smoke spreads to the inside, but the location that has already passed the vent (fire source 6-1-1) seems to cause the smoke to spread past the vent due to inertia. Therefore, to remove all the smoke spreading through the vent, the capacity of the 6 exhaust fan needs to be improved, which shows a similar tendency to the 6-1-2 fire source. In summer, when the exhaust fan is operated in the 6-3 fire source, the high-temperature smoke spreads from the fire source to vents 7 and 8. In winter, when the exhaust fan is operated, high-temperature smoke is exhausted through 6 vents, but when it is not operated, the smoke spreads to sections 7 and 8. (Figure 9) That is, when a fire occurs at this location of the fire source, the fan must not be operated in the summer, and the fan must be operated in the winter, unlike the field operation method.

The vent 7∼8 section has an upward-sloping structure in the direction of vent 8, and in the summer, when a fire breaks out in the 7-0 fire source, smoke can be seen spreading from the fire source toward vent 8. Even when the fan is not

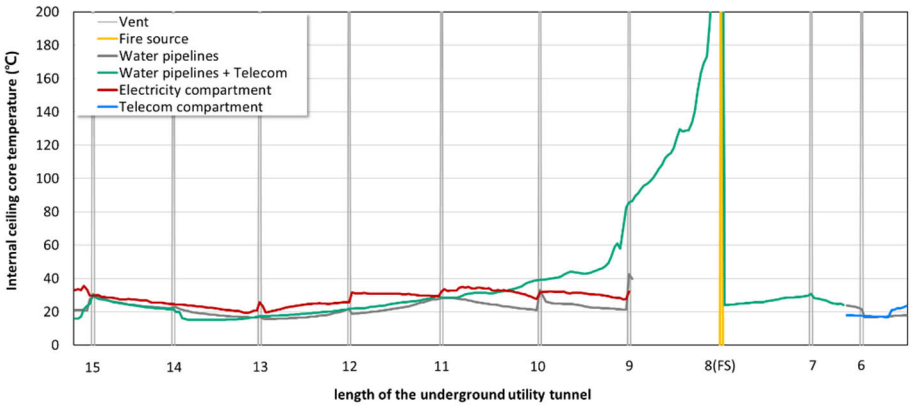

Vent	15	14	13	12	11	10	9	8	7	6
VFR (CMS)	3.82	-5.04	0.69	-4.71	2.17	-5.34	3.16	-1.47	8.48	-4.35
Temp (℃)	32.00	20.98	32.00	23.01	32.00	37.81	32.00	93.73	32.00	18.21

(a)

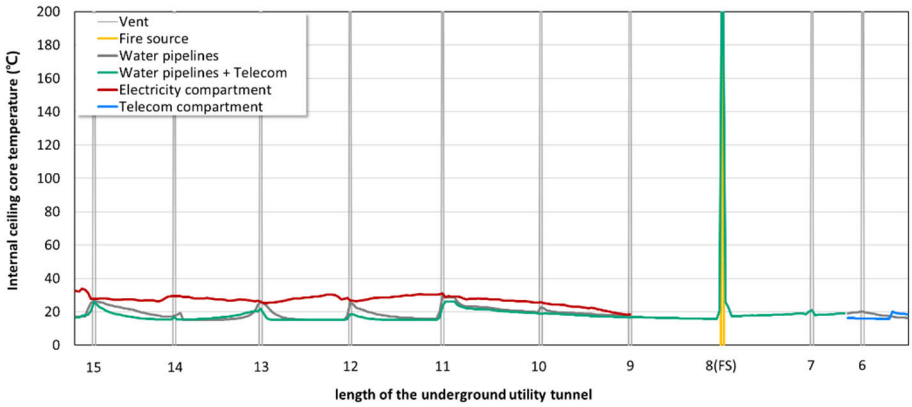

Vent	15	14	13	12	11	10	9	8	7	6
VFR (CMS)	-0.45	-1.80	3.90	0.33	3.11	-0.24	-0.02	-8.23	0.51	3.94
Temp (℃)	21.38	32.00	29.24	27.28	23.85	32.00	31.93	111.78	31.99	20.46

(b)

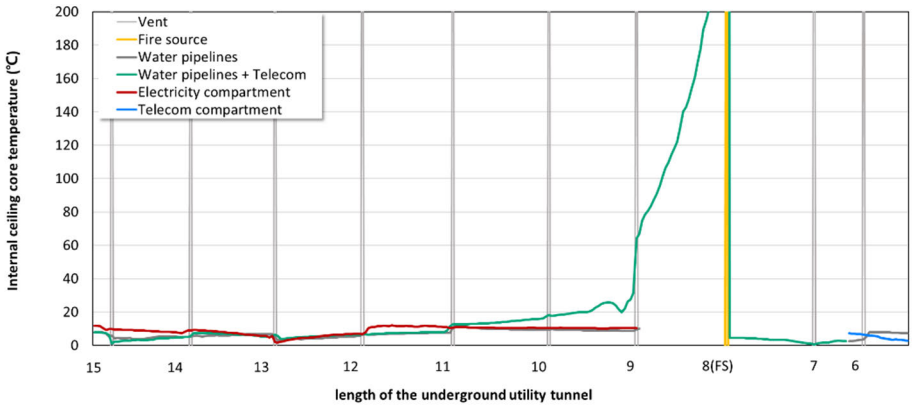

Vent	15	14	13	12	11	10	9	8	7	6
VFR (CMS)	6.21	-5.04	4.87	-4.71	-2.10	-5.34	2.24	-1.47	8.67	-4.35
Temp (℃)	0.00	5.08	0.00	6.10	8.10	16.60	0.00	219.29	0.00	3.91

(c)

FIGURE 13. Internal ceiling core temperature in case of fire source at 8-0: (a) Summer, fans working (b) Summer, fans not working (c) Winter, fans working (d) Winter, fans not working.

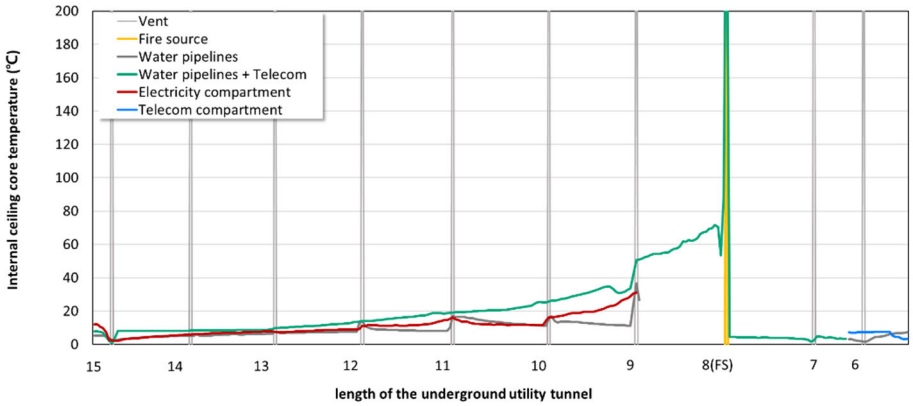

Vent	15	14	13	12	11	10	9	8	7	6
VFR (CMS)	5.84	-1.91	-3.32	-4.69	-5.31	-5.36	3.70	4.23	3.84	2.58
Temp (℃)	0.00	7.62	7.23	11.01	20.22	28.42	0.00	0.00	0.00	0.00

(d)

FIGURE 13. ***(Continued.)*** **Internal ceiling core temperature in case of fire source at 8-0: (a) Summer, fans working (b) Summer, fans not working (c) Winter, fans working (d) Winter, fans not working.**

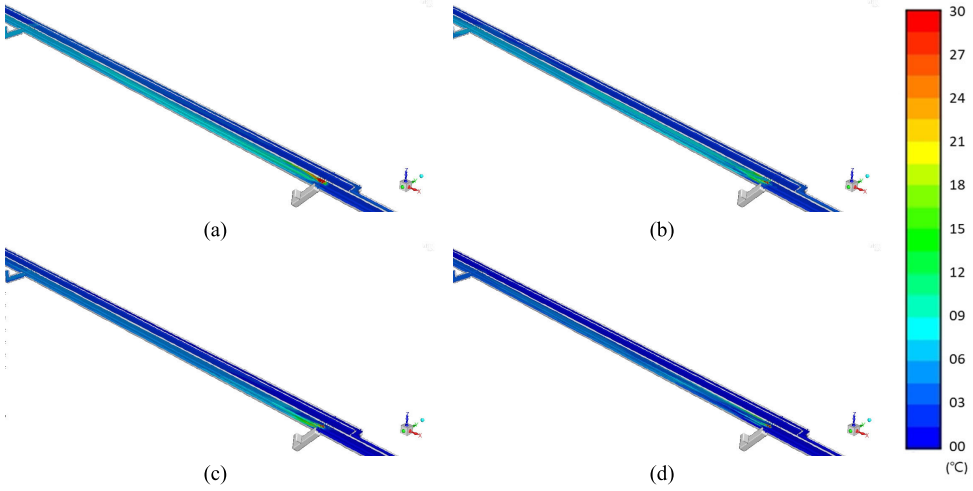

FIGURE 14. **Air temperature distribution inside underground utility tunnel in case of fire source at 9-0: (a) Summer, fans working (b) Summer, fans not working (c) Winter, fans working (d) Winter, fans not working.**

operated in the summer, vents 8 to 12 all operate as exhaust vents, and due to the natural force generated according to the structure, it tends to spread to vent 8. (Figure 10) When the fan is not operating in winter, the smoke spreads from the fire source toward vent 8. When the fan is running, all the fans are operated simultaneously, so even if the smoke can be exhausted naturally to vent 7 due to the flow generated by the exhaust fan 6, the smoke spreads out of the section. Regardless of whether the exhaust fan is operating or not, the smoke rises in an upward gradient, but it seems that the capacity of the 8 exhaust fan is insufficient compared to other vents, so all the smoke rising in an upward gradient cannot be exhausted. (Figure 11) However, in the case of winter, some smoke spreads to the 6 exhaust fan when the fan is operating, so in the case of a fire in this section, stopping all fans will help prevent the spread of smoke inside. In the 7-1 and 7-2 fire sources, the summer season shows the same tendency as the 7-0.

In the summer, when the fan at the 8-0 fire center is turned on, and smoke can be seen expanding in the direction toward vent 9. (Figure 12) This is because, as in the previous section, the vent 8-9 section has a gradient change section. After all, there is a collecting well between the sections, but the overall structure is a single slope. When the fan was not running, the exhaust through the 8 exhaust vents was 8.23 m^3/s, and all the smoke was exhausted. In winter, when the fan is not running, smoke can be seen extending from the fire source toward vent 9. When a fire occurs near the vent due to the small capacity of the exhaust fan 8, the natural ventilation is larger than the exhaust by the fan, so not operating the

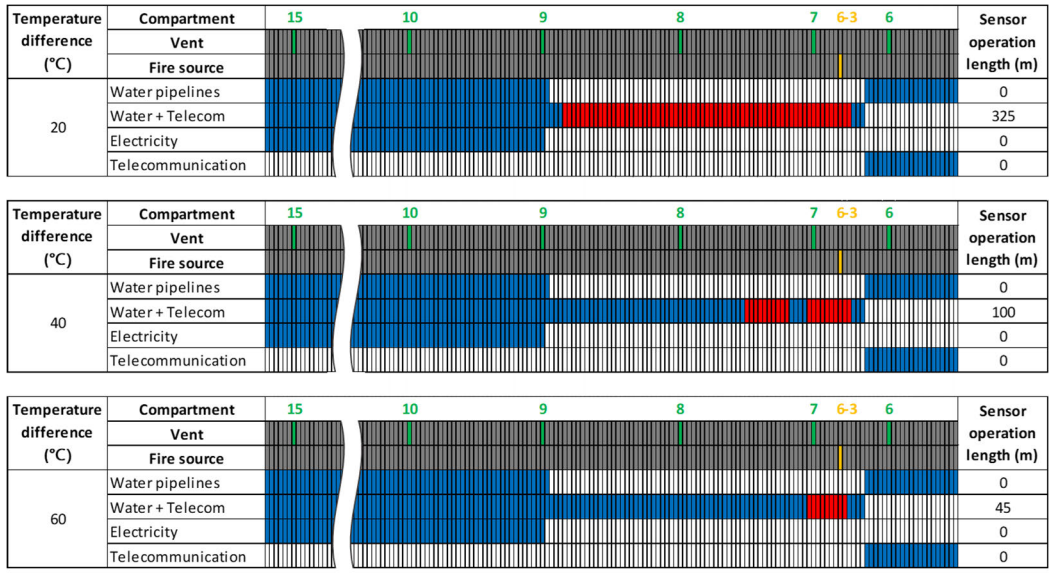

(a)

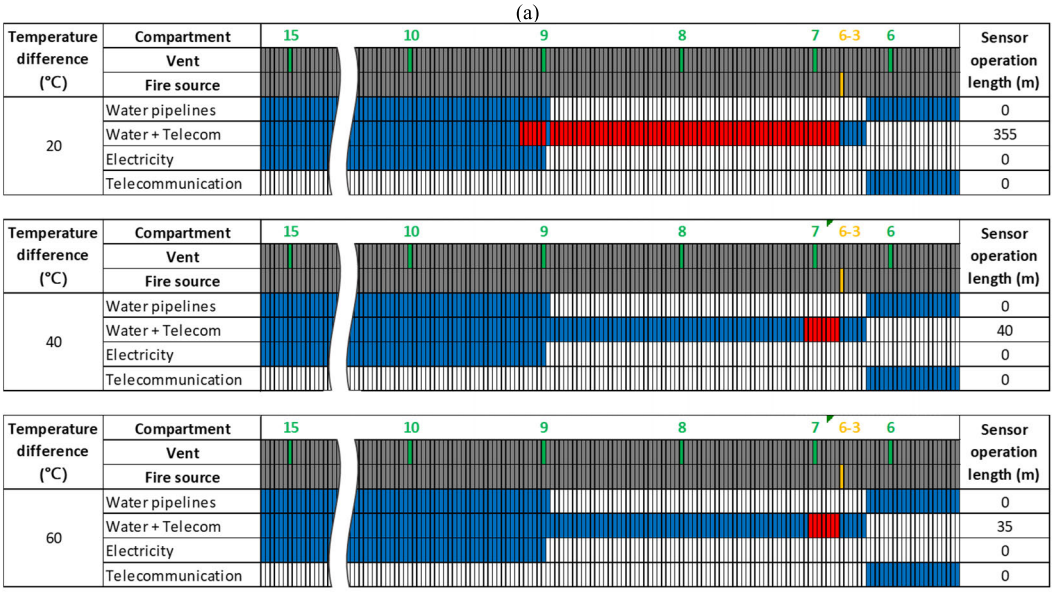

(b)

FIGURE 15. Operation section of fire detection sensor in case of fire source at 6-3: (a) Summer, fans working, (b) Winter, fans not working.

fan is advantageous in preventing smoke spread. (Figure 13) In the case of a fire in the 8-1 and 8-2 fire sources, smoke spreads from the fire source toward vent 9 during the summer season.

The section between vent 9 and 10 extends from a single track to three tracks, vent 9 is located in the single-track section and vent 10 is connected to the opposite side of the electricity compartment, which is the research area. The section gradient is a single gradient structure upward to vent 10. When a fire breaks out in the 9-0 fire source under all conditions, it can be seen that the smoke spreads in the direction from the fire source toward vent 10. Whether or not the exhaust fan 10 is operating does not affect overall smoke control. (Figure 14) Because vents 10 and 11 are located on the opposite side of the fire. Also, this is because the exhaust fan 12 is large and the vent is broad, so in the event of a fire in the electricity compartment, most of the smoke moves in an upward gradient direction along the electricity compartment. Whether the exhaust fan 10 is running does not affect the overall smoke removal. (Figure 14) In the case of fire source in 9-1 and 9-2, in all cases, high-temperature smoke spreads from the fire source toward vent 10. The exhaust fan 10, close to the upper gradient, is connected to the opposite side of the utility tunnel, and most of the smoke flows along the electricity compartment. It is exhausted to the outside through fan 12. However, the smoke diffused from the central part of

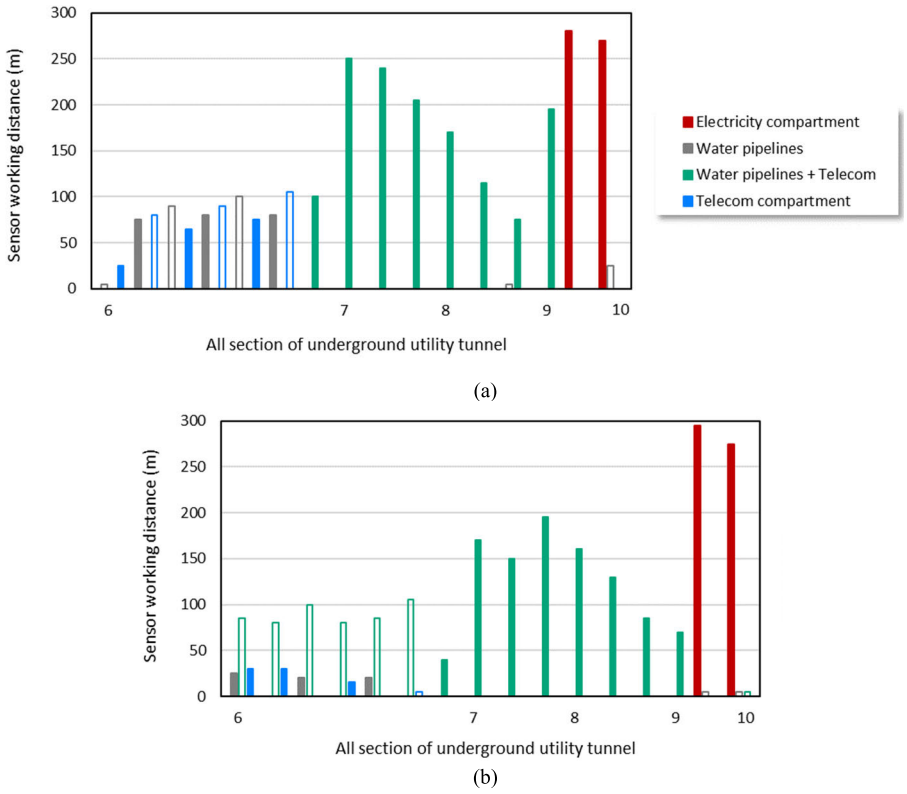

FIGURE 16. Sensor working distance by section according to seasonal fan operation: (a) Summer (b) Winter.

the ceiling of vent 10 appears to be at a high temperature, even on the non-fired side.

C. ANALYSIS OF SENSOR INSTALLATION FOR FIRE DETECTION

The operating length of the detection sensor is shown in Figure 15 by dividing the section into 5m spacing intervals, red when the temperature exceeds the regular times temperature, and blue when the temperature is below the temperature. The location of the vent and the location of the fire source are indicated so that the direction in which smoke spreads from the fire source can be determined. If the detects a slight temperature difference (20°C) compared to the temperature at normal times, the response to the temperature may be quick. However, it may be difficult to determine the location because several sections may be operated by high-temperature smoke propagated from the double-track section. In the case of detecting high-temperature difference (60°C), the detection length is shortened, so the sensors must be installed more densely, and it takes too long to detect danger, which is unfavorable for early detection of fire. It is analyzed that it is reasonable to detect 40°C compared to the temperature at regular times for fire detection.

In order to calculate the optimal number of sensors for fire detection by section between vents, the sensor operating distance was simulated for each section based on a temperature difference of 40°C compared to regular. (Figure 16) Since the minimum distance is required to detect all of the farther distances, the minimum value for each section was calculated for each season. In the section not included in the target section, only the outer line is displayed. The minimum distance of the total 4 sections is the location of fire source 6-1 in the winter (vent 6∼7), location 7-1 in the winter (vent 7∼8), location 8-2 in the summer (vent 8∼9), and location 9-2 in the summer (vent 9∼10), and each distance is shown in Table 7. The suggested sensor spacing is half of the minimum sensor operating distance. This is because at least two sensors must be installed at the minimum sensor working distance calculated above to detect a section that is not a point. The minimum number of sensors for fire detection was calculated by dividing the distance between vents by the minimum sensor operation distance. The section of vent 6∼7 has a gradient change, so more dense installation is required, so installing at 20m intervals seems necessary, which is half of the 40m distance detected in the 6-3 winter. In the case of vent 7∼10, the minimum detection distance is 75 m of the 8-2 location. So, it is analyzed that the position and direction of the fire can be detected if detected at an interval of about 30 m, which is half of this distance. In the case of a fire that occurs in front of a vent, the smoke is not spread to the left and right but is smoked directly through the vent. As a result of calculating each section by installing one detection sensor in each vent, at least 22 sensors are required.

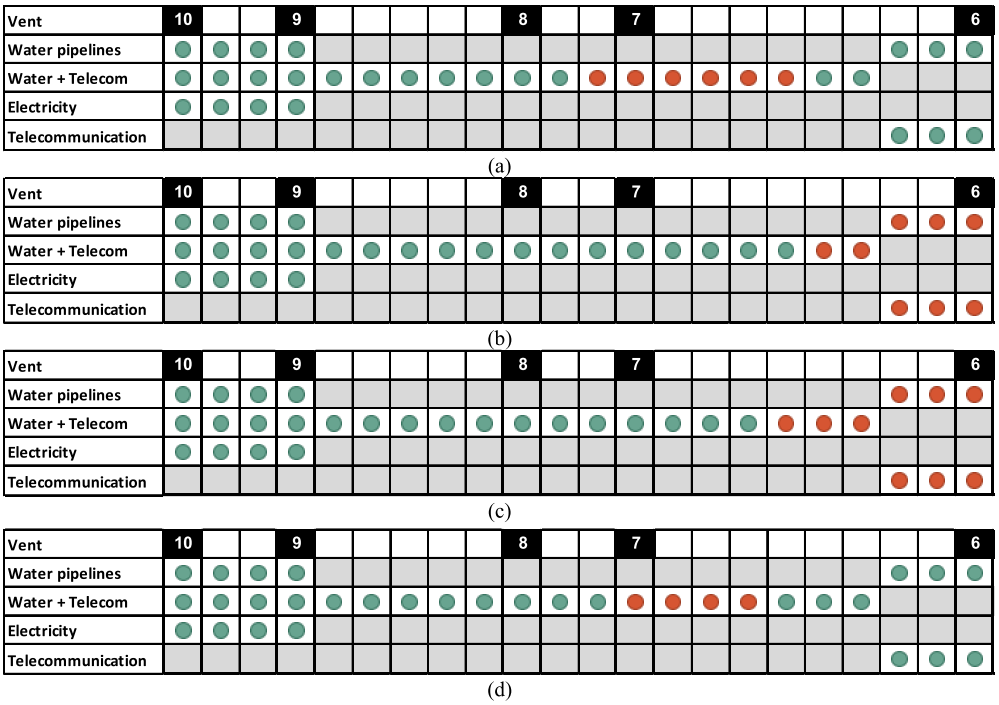

FIGURE 17. Sensor working distance by section according to seasonal fan operation in case of fire source at 6-3: (a) Summer, fans working (b) Summer, fans not working (c) Winter, fans working (d) Winter, fans not working.

D. EXHAUST FAN OPERATION FOR SMOKE EXTRACTION

In order to secure an access road when a fire breaks out in the target utility tunnel, an exhaust fan operation manual was derived to remove high-temperature smoke that spreads only a short section efficiently. When the results of the ventilation fan operation are the same, operating the fan in summer and not operating the fan in winter were calculated as the primary operation method of the field site. As shown in Figure 15, the high-temperature sensor detects high-temperature smoke extending from the fire source to vent 7, so the location of the fire source can be estimated as 6-3, which is close to vent 7. According to the results of Figure 17, in case of fire, not operating the fan in summer is more efficient for smoke exhaustion than operating the fan in the summer, and similarly, not operating the fan in the winter is more efficient. That is, it may be different from the operation method of the existing target underground utility tunnel. By installing the minimum number of sensors, the location of the fire source is quickly detected, and the result of determining whether to operate the exhaust fan for smoke removal is presented. This varies depending on the season and the location of the fire source. If the structure and exhaust fan design standards of the underground utility tunnel are established, it is expected that the following ventilation fan operation manual can be presented to respond quickly to fire.

IV. CONCLUSION

This study derived the optimum sensor location for detecting fire and fan operation for smoke removal by considering the ventilation system in the target underground utility tunnel. This study can guide the response manual for underground utility tunnels in case of fire. If the design drawings of the underground utility tunnel are standardized, it is expected to prevent significant damage. The main conclusions are as follows:

- The measured flow rate was less than the design flow rate. Because the exhaust outlet is blocked by the vent's vertical tunnel structure, the reason is due to the aging of the fan.
- When the exhaust fan is not operating, the heat diffusion is dominated by the inclined structure. When the fan is operating, it depends on the capacity of the surrounding fan from the fire source. Underground utility tunnel design standards are established based on the ventilation time, but the exhaust fan capacity needs to be increased to prevent the spread of fire.
- When a temperature difference of 40°C or more compared to the temperature occurs at regular times, it is appropriate to regard it as fire detection. In addition, it was analyzed that areas with complex structures require more sensors for fire detection.
- In order to secure access roads for firefighters, it was determined whether or not to control the exhaust fan for each season so that the smoke spreads only in a short section. In some target sections, operating differently from the on-site operation situation of the underground utility tunnel was more helpful in removing the smoke.

REFERENCES

[1] K. Young-Chin and K. Jae-Mo, "Research on the installation and maintenance measures for stability improvement of common utility and," *Korean Geo-Environ. Soc.*, pp. 285–290, Sep. 2005. http://www.dbpia.co.kr/journal/articleDetail?nodeId=NODE00644222

[2] *Korea Fire Safety Standards*, Standard KFS 1252, 2019.

[3] L. Zardasti, N. Yahaya, A. Valipour, A. S. A. Rashid, and N. M. Noor, "Review on the identification of reputation loss indicators in an onshore pipeline explosion event," *J. Loss Prevention Process Industries*, vol. 48, pp. 71–86, Jul. 2017, doi: 10.1016/j.jlp.2017.03.024.

[4] H. S. Kim, I. J. Hwang, and J. K. Youn, "The characteristics of flow induced by fire in an underground utility tunnel," in *Proc. Korean Soc. Mech. Eng.*, 2002, pp. 2098–2103. [Online]. Available: http://www.dbpia.co.kr/journal/articleDetail?nodeId=NODE00910111

[5] J.-I. Lee, "A study on the fire prevention activities and suppression measures of utility-pipe conduit," *Korean Soc. Hazard Mitigation*, vol. 10, no. 4, pp. 63–68, 2010. [Online]. Available: https://scienceon.kisti.re.kr/srch/selectPORSrchArticle.do?cn=JAKO201030650219149

[6] K. Dongkyu, D. Yoon, and B. Ahn, "Assessment of ventilation performance of underground tunnel with the domestic and international standards by using computer simulation," *J. Korean Soc. Hazard Mitigation*, vol. 17, no. 3, pp. 79–86, 2017.

[7] H. Seo, H. Choi, M. C. Lee, and C. G. Song, "Establishing a risk assessment scenario for fire prevention and safety management in underground urban utility tunnels," *J. Korean Soc. Hazard Mitigation*, vol. 19, no. 1, pp. 241–248, Feb. 2019, doi: 10.9798/KOSHAM.2019.19.1.241.

[8] Y. Mouilleau and A. Champassith, "CFD simulations of atmospheric gas dispersion using the fire dynamics simulator (FDS)," *J. Loss Prevention Process Industries*, vol. 22, pp. 316–323, May 2009, doi: 10.1016/j.jlp.2008.11.009.

[9] P. Sharma, B. Gera, and R. Singh, "A CFD validation of fire dynamics simulator for corner fire," *CFD Lett. Int. J.*, vol. 2, no. 4, pp. 137–148, 2010.

[10] J. Glasa, L. Valasek, P. Weisenpacher, and L. Halada, "Cinema fire modelling by FDS," *J. Phys. Conf. Ser.*, vol. 410, Feb. 2013, Art. no. 012013, doi: 10.1088/1742-6596/410/1/012013.

[11] F. Fernández-Alaiz, A. M. Castañón, F. Gómez-Fernández, and M. Bascompta, "Mine fire behavior under different ventilation conditions: Real-scale tests and CFD modeling," *Appl. Sci.*, vol. 10, no. 10, p. 3380, May 2020, doi: 10.3390/app10103380.

[12] P. Bernardi, E. Michelini, A. Sirico, S. Rainieri, and C. Corradi, "Simulation methodology for the assessment of the structural safety of concrete tunnel linings based on CFD fire—FE thermo-mechanical analysis: A case study," *Eng. Struct.*, vol. 225, Dec. 2020, Art. no. 111193, doi: 10.1016/j.engstruct.2020.111193.

[13] K. Chul-Soo, L. Won-Sup, and K. Hong-Sik, "The characteristics of flow induced by fire in an underground utility tunnel," *J. Korean Soc. Mech. Technol.*, vol. 5, no. 1, pp. 59–64, 2003. [Online]. Available: https://www.earticle.net/Article/A20309

[14] K. Liang, X. Hao, W. An, Y. Tang, and Y. Cong, "Study on cable fire spread and smoke temperature distribution in T-shaped utility tunnel," *Case Stud. Thermal Eng.*, vol. 14, Sep. 2019, Art. no. 100433, doi: 10.1016/j.csite.2019.100433.

[15] An, Y. Tang, K. Liang, C. Minglun, T. Wang, and Z. Wang, "Study on temperature distribution and CO diffusion induced by cable fire in L-shaped utility tunnel," *Sustain. Cities Soc.*, vol. 62, Jul. 2020, Art. no. 102407, doi: 10.1016/j.scs.2020.102407.

[16] X. Guo, X. Pan, Z. Wang, J. Yang, M. Hua, and J. Jiang, "Numerical simulation of fire smoke in extra-long river-crossing subway tunnels," *Tunnelling Underground Space Technol.*, vol. 82, pp. 82–98, Dec. 2018.

[17] H. Zhang and Y. Zhao, "Study on underground utility tunnel fire characteristics under sealing and ventilation conditions," *Adv. Civil Eng.*, vol. 2020, pp. 1–11, Jan. 2020, doi: 10.1155/2020/9128704.

[18] R. Hasib, R. Kumar, Shashi, and S. Kumar, "Simulation of an experimental compartment fire by CFD," *Building Environ.*, vol. 42, no. 9, pp. 3149–3160, Sep. 2007, doi: 10.1016/j.buildenv.2006.08.002.

[19] K.-J. Park, K.-J. Lee, B. E. Hadi, J.-H. Lee, and D.-I. Shin, "Smoke control according to the ventilation capacity in subway tunnel fire: I. FDS simulation," *J. Korean Inst. Gas*, vol. 15, no. 3, pp. 31–38, Jun. 2011. [Online]. Available: https://kiss.kstudy.com/Detail/Ar?key=2930707

[20] E. Dobrucali, "Theoretically investigation of smoke production in a tunnel fire," *J. Naval Sci. Eng.*, vol. 9, p. 18, Apr. 2013.

[21] L. Sang-Eun and L. Chang-Woo, "Construction of the smoke exhaust system and its applicability by the fire model test for a bidirectional tunnel," *Tunnel Underground Space*, vol. 15, no. 6, pp. 452–461, 2005. [Online]. Available: http://www.dbpia.co.kr/journal/articleDetail?nodeId=NODE01030492

[22] Y. Yongho, "The smoke extraction efficiency improvement by the partial extraction system in tunnel fire," in *Proc. Korean Soc. Fluid Machinery*, 2006, pp. 801–804. [Online]. Available: http://www.dbpia.co.kr/journal/articleDetail?nodeId=NODE01172574

[23] H. B. Kim, Y. J. Jang, W. S. Jung, and W. H. Park, "Comparative study on the numerical simulation for the tunnel fire driven flow with the turbulence model in RANS and LES method in FDS code," *Korean Soc. Mech. Eng.*, pp. 229–234, 2007. [Online]. Available: http://www.dbpia.co.kr/journal/articleDetail?nodeId=NODE00915779

[24] J.-Y. Kim and J.-O. Yoo, "A numerical study on characteristics of smoke exhaust in road tunnel fires for different ventilation system," *FIRE Sci. Eng.*, vol. 22, no. 3, pp. 201–207, 2008. [Online]. Available: https://scienceon.kisti.re.kr/srch/selectPORSrchArticle.do?cn=JAKO200833338746664

[25] Y.-C. K. Shin, L. Soo-Young, K. Ju-Hee, and I. Young-Jin, "An experimental and analytical studies on the smoke movement by fire," in *Proc. Korea Inst. Fire Sci. Eng. Conf.*, South Korea, 2008, p. 15.

[26] J. C. Edwards and C. C. Hwang, "Mining publication: CFD modeling of fire spread along combustibles in a mine entry," in *Proc. SME Annu. Meeting Exhib.*, 2006, pp. 1–5.

[27] A. Amouzandeh, M. Zeiml, and R. Lackner, "Real-scale CFD simulations of fire in single- and double-track railway tunnels of arched and rectangular shape under different ventilation conditions," *Eng. Struct.*, vol. 77, pp. 193–206, Oct. 2014, doi: 10.1016/j.engstruct.2014.05.027.

[28] M. G. M. van der Heijden, M. G. L. C. Loomans, A. D. Lemaire, and J. L. M. Hensen, "Fire safety assessment of semi-open car parks based on validated CFD simulations," *Building Simul.*, vol. 6, no. 4, pp. 385–394, Dec. 2013, doi: 10.1007/s12273-013-0118-7.

[29] T. Baalisampang, R. Abbassi, V. Garaniya, F. Khan, and M. Dadashzadeh, "Modelling the impacts of fire in a typical FLNG processing facility," in *Proc. Int. Conf. Safety Fire Eng.*, 2017.

[30] T. Yamada and Y. Akizuki, "Visibility and human behavior in fire smoke," in *SFPE Handbook of Fire Protection Engineering*, vol. 16, no. 3. 2016, pp. 2181–2206.

[31] K. Jeongsoo, L. Chan-Woo, P. Seung-Hwa, L. Jong-Hyun, and H. Chang-Hee, "Development of fire detection model for underground utility facilities using deep learning: Training data supplement and bias optimization," *J. Korea Academia-Ind. Cooperation Soc.*, vol. 21, no. 12, pp. 320–330, 2020. [Online]. Available: http://www.dbpia.co.kr/journal/articleDetail?nodeId=NODE10509878

[32] T. Baalisampang, R. Abbassi, V. Garaniya, F. Khan, and M. Dadashzadeh, "Fire impact assessment in FLNG processing facilities using computational fluid dynamics (CFD)," *Fire Saf. J.*, vol. 92, pp. 42–52, Sep. 2017, doi: 10.1016/j.firesaf.2017.05.012.

[33] L. Byung-Jin, P. Chul-Woo, L. Mi-Suk, and J. Woo-Sug, "Development of a acoustic acquisition prototype device and system modules for fire detection in the underground utility tunnel," *J. Inst. Internet, Broadcast. Commun.*, vol. 22, no. 5, pp. 7–15, 2022. [Online]. Available: https://www.earticle.net/Article/A419579

[34] D. Willemann and J. G. Sanchez, "Computer modeling techniques and analysis used in design of tunnel ventilation fan plants for the New York City subway," in *Proc. ASME/IEEE Joint Railroad Conf.*, Apr. 2002, pp. 73–80.

[35] K. Dongkyu, "A study on the method of air velocity calculations for ventilation performance in the underground utility tunnels using FDS," M.S. thesis, Dept. Building Equip., Gachon Univ., Seongnam, South Korea, 2016. [Online]. Available: http://www.riss.kr/link?id=T14006142

[36] W. Wang, Z. Zhu, Z. Jiao, H. Mi, and Q. Wang, "Characteristics of fire and smoke in the natural gas cabin of urban underground utility tunnels based on CFD simulations," *Tunnelling Underground Space Technol.*, vol. 109, Mar. 2021, Art. no. 103748, doi: 10.1016/j.psep.2020.11.036.

[37] T. Baalisampang, E. Saliba, F. Salehi, V. Garaniya, and L. Chen, "Optimisation of smoke extraction system in fire scenarios using CFD modelling," *Process Saf. Environ. Protection*, vol. 149, pp. 508–517, May 2021, doi: https://doi.org/10.1016/j.pSep. 2020.11.036.

[38] H. Zhu, Y. Shen, Z. Yan, Q. Guo, and Q. Guo, "A numerical study on the feasibility and efficiency of point smoke extraction strategies in large cross-section shield tunnel fires using CFD modeling," *J. Loss Prevention Process Industries*, vol. 44, pp. 158–170, Nov. 2016, doi: 10.1016/j.jlp.2016.09.005.

[39] H. Mi, Y. Liu, Z. Jiao, W. Wang, and Q. Wang, "A numerical study on the optimization of ventilation mode during emergency of cable fire in utility tunnel," *Tunnelling Underground Space Technol.*, vol. 100, Jun. 2020, Art. no. 103403, doi: 10.1016/j.tust.2020.103403.

[40] S.-J. Park, I.-B. Lee, S.-Y. Lee, J.-G. Kim, J.-H. Cho, C. Decano-Valentin, Y.-B. Choi, M.-H. Lee, H.-H. Jeong, U.-H. Yeo, W.-S. Jung, and D.-Y. Jeong, "Air conditioning system design to reduce condensation in an underground utility tunnel using CFD," *IEEE Access*, vol. 10, pp. 116384–116401, 2022, doi: 10.1109/ACCESS.2022.3219210.
[41] J. Choi, "A study on the characteristics and the disaster prevention measures of incendiary fire," *Fire Sci. Eng.*, vol. 22, no. 5, 2008.
[42] T. Norton, J. Grant, R. Fallon, and D.-W. Sun, "Assessing the ventilation effectiveness of naturally ventilated livestock buildings under wind dominated conditions using computational fluid dynamics," *Biosystems Eng.*, vol. 103, no. 1, pp. 78–99, May 2009, doi: 10.1016/j.biosystemseng.2009.02.007.
[43] K.-S. Kwon, I.-B. Lee, G. Q. Zhang, and T. Ha, "Computational fluid dynamics analysis of the thermal distribution of animal occupied zones using the jet-drop-distance concept in a mechanically ventilated broiler house," *Biosystems Eng.*, vol. 136, pp. 51–68, Aug. 2015, doi: 10.1016/j.biosystemseng.2015.05.008.
[44] S. Kato, "Review of airflow and transport analysis in building using CFD and network model," *Jpn. Architectural Rev.*, vol. 1, pp. 299–309, Jul. 2018, doi: 10.1002/2475-8876.12051.
[45] S. Zhang, A. Ding, X. Zou, B. Feng, X. Qiu, S. Wang, S. Zhang, Y. Qian, H. Yao, and Y. Wei, "Simulation analysis of a ventilation system in a smart broiler chamber based on computational fluid dynamics," *Atmosphere*, vol. 10, no. 6, p. 315, Jun. 2019, doi: 10.3390/atmos10060315.
[46] M. Lee, G. Park, H. Jang, and C. Kim, "Development of building CFD model design process based on BIM," *Appl. Sci.*, vol. 11, no. 3, p. 1252, Jan. 2021, doi: 10.3390/app11031252.
[47] A. Hellsten, "New two-equation turbulence model for aerodynamics applications," Doctoral thesis, Helsinki Univ. Technol., Espoo, Finland, 2014. [Online]. Available: http://urn.fi/urn:nbn:Fi:tkk-003332
[48] B. Godderidge, M. Tan, S. R. Turnock, and C. Earl, "A verification and validation study of the application of computational fluid dynamics to the modelling of lateral sloshing," Univ. Southampton, Southampton, U.K., Ship Sci. Rep. 140, 2006, p. 158.
[49] F. Gao, H. Wang, and H. Wang, "Comparison of different turbulence models in simulating unsteady flow," *Proc. Eng.*, vol. 205, pp. 3970–3977, Jan. 2017, doi: 10.1016/j.proeng.2017.09.856.
[50] S. Galván, M. Reggio, and F. Guibault, "Assessment study of K-ε turbulence models and near-wall modeling for steady state swirling flow analysis in draft tube using fluent," *Eng. Appl. Comput. Fluid Mech.*, vol. 5, no. 4, pp. 459–478, 2011, doi: 10.1080/19942060.2011.11015386.
[51] P. Mishra and K. R. Aharwal, "A review on selection of turbulence model for CFD analysis of air flow within a cold storage," *IOP Conf. Ser., Mater. Sci. Eng.*, vol. 402, no. 1, 2018, Art. no. 012145, doi: 10.1088/1757-899X/402/1/012145.
[52] K. Ye, X. Zhou, L. Yang, X. Tang, Y. Zheng, B. Cao, Y. Peng, H. Liu, and Y. Ni, "A multi-scale analysis of the fire problems in an urban utility tunnel," *Energies*, vol. 12, no. 10, p. 1976, May 2019, doi: 10.3390/en12101976.
[53] *National Fire Safety Code*, NFSC 203, 2013. [Online]. Available: https://www.law.go.kr/LSW/admRulLsInfoP.do?vSct=NFSC+203&admRulSeq=2100000178589 and https://www.scribbr.com/apa-examples/law/

JEONG-HWA CHO received the B.S. degree from the Department of Biosystems Engineering, Chungbuk National University, in 2015, and the M.S. degree from the Department of Mechanical Engineering, Chungnam National University, in 2018. She is currently pursuing the Ph.D. degree with Seoul National University, Seoul, South Korea. Recently, she is studying agricultural engineering for urban agriculture. Her research interests include aero-environment, energy saving of facilities, HVAC evaluation and design, and atmospheric diffusion.

IN-BOK LEE received the B.S. degree from the Department of Agricultural Engineering, Konkuk University, in 1987, and the M.S. and Ph.D. degrees from the Department of Agricultural Engineering, The Ohio State University (OSU), USA, in 1995 and 1998, respectively. Since 2005, he has been a Faculty Member with the Department of Rural Systems Engineering, Seoul National University. His research interests include aero-environment and energy saving of smart farms, such as greenhouses, livestock houses, and storages, while being very active in applying advanced ICT technologies to smart farms.

WOO-SUG JEONG received the B.S. and M.S. degrees in electronics engineering from Myongji University, Seoul, South Korea, in 1992 and 1994, respectively, and the Ph.D. degree in computer engineering from Chungnam University, Daejeon, South Korea. Since 1994, he has been a Researcher in the field of various IT technologies, such as network equipment, the IoT, and AR/VR. He is currently the Director of the Disaster and Safety AI Convergence Center, ETRI. He is conducting research in the disaster safety field with IT technology for safe social construction. His research interests include digital twin, metaverse, networks, the IoT, AR/VR, and the disaster safety field.

BYUNG-JIN LEE received the B.S. degree in information and communication engineering and the combined M.S. and Ph.D. degree in radio communication engineering from Chungbuk University, Cheongju, South Korea, in 2013 and 2019, respectively. From 2019 to 2021, he researched on acoustic signal processing, the IoT, and AI with the KT Institute of Convergence Technology. He is currently a Senior Researcher with the Disaster and Safety AI Convergence Center, ETRI. He is conducting research in the disaster safety field with IT technology for safe social construction. His research interests include digital twins, metaverse, digital signal processing, AI, and disaster safety field.